THE JOURNAL OF BIOLOGICAL CHEMISTRY Vol. 277, No. 46, Issue of November 15, pp. 44385–44398, 2002
Printed in U.S.A.

Deciphering Vascular Endothelial Cell Growth Factor/Vascular Permeability Factor Signaling to Vascular Permeability

INHIBITION BY ATRIAL NATRIURETIC PEPTIDE*

Received for publication, March 12, 2002, and in revised form, August 27, 2002
Published, JBC Papers in Press, September 3, 2002, DOI 10.1074/jbc.M202391200

Ali Pedram‡, Mahnaz Razandi‡, and Ellis R. Levin‡§¶

From the Division of Endocrinology, Veterans Affairs Medical Center, Long Beach, California 90822 and Departments of ‡Medicine and §Pharmacology, University of California, Irvine, California 92717

Vascular endothelial cell growth factor (VEGF) was originally described as a potent vascular permeability factor (VPF) that importantly contributes to vascular pathobiology. The signaling pathways that underlie VEGF/VPF-induced permeability are not well defined. Furthermore, endogenous vascular peptides that regulate this important VPF function are currently unknown. We report here that VPF significantly enhances permeability in aortic endothelial cells via a linked signaling pathway, sequentially involving Src, ERK, JNK, and phosphatidylinositol 3-kinase/AKT. This leads to the serine/threonine phosphorylation and redistribution of actin and the tight junction (TJ) proteins, zona occludens-1 and occludin, and the loss of the endothelial cell barrier architecture. Atrial natriuretic peptide (ANP) inhibited VPF signaling, TJ protein phosphorylation and localization, and VPF-induced permeability. This involved both guanylate cyclase and natriuretic peptide clearance receptors. *In vivo*, transgenic mice that overexpress ANP showed significantly less VPF-induced kinase activation and vascular permeability compared with non-transgenic littermates. Thus, ANP acts as an anti-permeability factor by inhibiting the signaling functions of VPF that we define here and by preserving the endothelial cell TJ functional morphology.

The vascular endothelial cell growth factor (VEGF)[1] glycoprotein is an important angiogenesis factor that was originally isolated as a vascular permeability factor (VPF) (1, 2). VEGF/VPF (henceforth designated VPF) potently stimulates fluid transgression through endothelial cell (EC) tight junctions (TJ) (3, 4). This permeability factor also modulates the formation and function of vesiculovascular organelles in venules (5) and the development of EC fenestrations (6). These mechanisms underlie the enhanced vascular permeability seen in response to VPF, which is implicated in the ascites associated with ovarian and other carcinomas (1, 7), the pathogenesis of diabetic retinopathy (8), and the ovarian hyperstimulation syndrome (9).

The angiogenesis-promoting actions of VPF result after binding and signaling through the transmembrane receptors Flk-1 (10), Flt-1 (11), and neuropilin (12). The Flk-1 tyrosine kinase receptor (VEGF-R2) has been proposed to participate in VPF permeability (13), but signaling through other related receptors also appears to be important (14). Flk-1 receptors activate membrane-associated kinases, such as Src and phosphatidylinositol 3-kinase (PI3K) (11, 15), and Src is critical to the role of the participation of VPF in the development of local edema following brain insult (16, 17). PI3K contributes to the ability of VPF to promote EC migration (18), but its precise role in permeability is unclear. Signaling to the generation of nitric oxide (NO) (13, 18) and subsequent activation of the extracellular signal-regulated kinase (ERK), mitogen-activated protein kinase (19), prostacyclin generation (13), or VPF-induced protein kinase C activity (20) have all been proposed to contribute to increased vascular permeability. How activation of various signals is integrated into a functional pathway responsible for permeability is undetermined.

Regarding NO, this gas disrupts both cytoskeletal protein complexing in epithelial cells and the arrangement of the actin cytoskeleton (21–24). This results in the dilation of cell tight junctions due to ATP depletion (23). We previously implicated NO as participating in VPF-induced permeability in the pathogenesis of the human ovarian hyperstimulation syndrome (9). In parallel, poorly defined VPF signaling pathways can result in the phosphorylation of TJ proteins that exist in complex, such as zona occludens-1 (ZO-1) or occludin (24). Phosphorylation of TJ proteins results in a lower transcellular resistance of EC (25), serving as an index of barrier function. Upon phosphorylation, TJ proteins assume abnormal relationships with other members of this complex, thereby creating "leaky" endothelial cell-cell contacts (26, 27). Thus, VPF-induced signaling to the cytoskeleton and to associated TJ proteins is potentially important and could present therapeutic targets to prevent vascular pathobiology (7–9).

Relevant to vascular biology, the natriuretic peptides (NP) are a family of small proteins that modulate salt and water balance, as well as vascular tone (reviewed in Ref. 28). Atrial and brain natriuretic peptides (ANP and BNP) are produced predominantly in the heart, whereas C-type natriuretic peptide (CNP) is synthesized by the endothelial cell. These peptides inhibit vascular cell growth mainly after binding the guanylate cyclase A (reactive to ANP or BNP) or B (CNP specific) recep-

* This work was supported by grants from the Research Service of the Department of Veterans Affairs and National Institutes of Health Grant HL-59890 (to E. R. L.). The costs of publication of this article were defrayed in part by the payment of page charges. This article must therefore be hereby marked "*advertisement*" in accordance with 18 U.S.C. Section 1734 solely to indicate this fact.

¶ To whom correspondence should be addressed: Medical Service (11/111-I), Long Beach Veterans Affairs Medical Center, 5901 E. 7th St., Long Beach, CA 90822. Tel.: 562-494-5748; Fax: 562-494-5515; E-mail: ellis.levin@med.va.gov.

[1] The abbreviations used are: VEGF, vascular endothelial cell growth factor; ANP, atrial natriuretic peptide; CNP, C-type natriuretic peptide; ERK, extracellular signal-regulated kinase; JNK, c-Jun N-terminal kinase: NPRC, natriuretic peptide receptor, clearance; NO, nitric oxide; PI3K, phosphatidylinositol 3-kinase; TJ, tight junction; VPF, vascular permeability factor; ZO, zona occludens; DMEM, Dulbecco's modified Eagle's medium; BAEC, bovine aortic endothelial cells; L-NAME, monomethyl L-arginine; EC, endothelial cell; BNP, brain natriuretic peptide; NP, natriuretic peptides; PKG, protein kinase G; MAP, mitogen-activated protein; ANOVA, analysis of variance.

tors (29, 30). This stimulates the production of cGMP and subsequent activation of PKG, inducing target genes or the modulation of K^+ channels (28). A second class of NP receptors is the clearance receptor (NPRC) (31), and this protein may contribute to the inhibition of cardiomyocyte, vascular endothelial cell, or astrocyte proliferation (28, 32, 33).

Because VPF-induced permeability underlies the pathobiology of several disorders (7–9, 16), we determined a relevant signaling pathway and the resulting morphological consequences in EC. Furthermore, we identify the NP as inhibitors of these processes, *in vitro* and *in vivo*.

EXPERIMENTAL PROCEDURES

Materials—Antibodies and substrate for kinase activation/activity and for phospho-ZO-1 or occludin were from Santa Cruz Biotechnology, Santa Cruz, CA. PD98059 was a generous gift from Dr. Alan Saltiel (Parke-Davis). VPF, wortmannin, LY294002, PP2, and L-NAME, and L-N^G-methyl-L-arginine acetate were from Calbiochem. LipofectAMINE was from Invitrogen. [^{3}H]Mannitol was from PerkinElmer Life Sciences. SB203580 was from Dr. P. R. Young (Smith Kline & French Laboratories) (34).

Cell Preparation—Primary cultures of bovine aortic EC were prepared and used as described previously (35, 36). In transfection studies, EC were generally used in passages 4–5, based upon previous observations that this greatly increases the transfection efficiency of these cells.

Kinase Activity Assays—For ERK and c-Jun N-terminal kinase (JNK) activity assays, the cells were synchronized for 24 h in serum- and growth factor-free medium. The cells were then exposed to VPF, 10–20 ng/ml, for 10 (ERK) or 15 min (JNK), with or without additional substances or peptides, as described previously (36, 37). Immunoprecipitated kinases were then added to the protein myelin basic protein (for ERK), or glutathione *S*-transferase-c-Jun-(1–79) (for JNK) for *in vitro* kinase assays. In addition, the VPF-induced phosphorylation of Src (8 min) and AKT (15 min) kinases were determined as indices of activation. Cultured cell lysates were pelleted and dissolved in SDS sample buffer, boiled, separated, and then transferred to nitrocellulose. Phosphorylated kinase proteins were detected using phospho-specific monoclonal antibodies (Santa Cruz Biotechnology) and the ECL Western blot kit. Equal samples from the cells were also immunoprecipitated, and immunoblots of the precipitated kinase protein from each experimental condition were determined to show equal gel loading. All experiments were repeated two to three times.

Transient Transfections—BAEC (passage 4–5) were grown to 40–50% confluence and then transiently transfected with 1.5 (each well of 6-well plates) or 10 μg of fusion plasmid DNA (100-mm dishes). Plasmids included wild type JNK-1 (pcDNA3FLAG-JNK-1) or dominant negative JNK-1 (pcDNA3 FLAG-JNK-1 APF) (kindly provided by Dr. Roger Davis) (38), dominant negative Myc-tagged pMT2-AH-AKT (kindly provided by Dr. Julian Downward) (39), dominant negative PI-3K p85 subunit (pcDNA3-Δp85, lacking residues 478–513) (kindly provided by Dr. Barry Posner) (40), dominant negative Src constructs pRC-cSrc-K298M (kindly provided by Drs. Louis Luttrell and Robert Lefkowitz) (41), and SrcK296R/Y528F (kindly provided by Michael Simonson) (42). Transfection was carried out using LipofectAMINE. Cells were incubated with liposome-DNA complexes at 37 °C for 5 h, followed by overnight recovery in DMEM containing 10% fetal bovine serum, 24 h synchronization in serum-free DMEM, and then treatment with VPF ± NP.

Endothelial Cell Permeability Assay—Assays were performed as described previously (9). Primary cultures of BAEC were seeded onto 0.45-μm CM filters (Millipore, Bedford, MA) within plastic inserts; the inserts were placed into 24-well plates, and the cells were grown to confluence over several days. In some experiments, the EC were first transfected with dominant negative constructs of JNK, PI3K, or Akt and then transferred to chambers. Chambers were created by placing medium inside the inner insert and the outer wells, with the endothelial cell monolayer on the insert filter. To both the apical and basolateral surface of the insert containing the cells on filter was added VPF ± 100 nM NP or other substances (see below). To the apical surface, 1 μl of [^{3}H]mannitol (1×10^6 cpm) was additionally added. These volumes equalized fluid heights in the two chambers, so that only diffusive forces would be involved in permeability of the BAEC. Flux rate was determined at 24 h by measuring the amount of [^{3}H]mannitol permeating to the basolateral compartment, determined by β-counting the aspirated well fluid. In some experiments, the nitric oxide synthase inhibitor, 1 μM monomethyl L-arginine (L-NAME), the ERK inhibitor, 1 μM PD98059, the p38 MAP kinase inhibitor, 1 μM SB203580, or an Src family kinase inhibitor, 50 μM PP2 (43), was added to EC cultures 30 min prior to the addition of VPF. DMEM culture media with and without labeled mannitol (no serum or added peptides) was used for control permeability assessments.

EC Monolayer Resistance Assay—Primary BAEC were grown until post-confluent on Transwell filters (Millicell) that were previously coated with rat tail collagen. The EC were then treated with VEGF ± ANP for 24 h. The electrical resistance of the filter-grown endothelial cell monolayers was measured using an EVOM resistance meter with Endohm Chamber (World Precision Instruments, Sarasota, FL). For measurements, both apical and basolateral sides of the endothelial cells were bathed with the same buffer solution (DMEM). Electrical resistance was recorded from probes inserted into the buffer inside and outside the chamber until similar values were reproducible on three consecutive measurements. The values of the EC monolayers are reported after subtracting the inherent resistance of the filters. Studies were carried out three times.

Cytoskeletal Actin—Non-transfected or transfected EC were grown to confluence on poly-D-lysine-coated glass coverslips and then exposed to 10 ng/ml VPF ± ANP or 100 nM C-ANP-(4–23) for 30 min. The cells were permeabilized, washed, then stained with fluorescent-labeled phalloidin (Molecular Probes). Actin distribution was examined and photographed under a Nikon epifluorescent microscope.

ZO-1 and Occludin Studies—The phosphorylation of ZO-1 or occludin was determined by Western blot. Subconfluent, transfected, or non-transfected cultured BAEC were serum-deprived overnight and then incubated under various conditions for 10 min with inhibitors followed by 30 min of treatment with stimulants. The cells were lysed and antibodies to ZO-1 or occludin (1:50 dilution) were conjugated to Sepharose beads and then added to the cell lysate for 2 h at 4 °C. After pelleting and washing, samples were electrophoretically separated on a 7% SDS gel, transferred to nitrocellulose, and immunoblotted. Detection utilized the ECL kit (Amersham Biosciences). For immunofluorescent staining of ZO-1 and occludin proteins, BAEC were cultured on coverslips in DMEM containing 10% fetal bovine serum. Upon confluence, coverslips were treated, fixed, and stained. BAEC coverslips were either pretreated with ANP or other inhibitors and then exposed to VEGF for 30 min. Cells were fixed in 2% freshly prepared paraformaldehyde for 10 min at room temperature, permeabilized with 0.1% Triton X-100 for 3 min, and then incubated with 0.5% bovine serum albumin in phosphate-buffered saline solution for 30 min at 23 °C. After washing, primary antibodies of mouse anti-occludin (1:250) and rabbit anti ZO-1 (1:250; Zymed Laboratories Inc., San Francisco, CA) were added for 1 h at 37 °C. Coverslips were then washed and fluorescently labeled secondary antibodies (1:200), anti-mouse fluorescein isothiocyanate, and anti-rabbit fluorescein isothiocyanate (Santa Cruz Biotechnology), were added at 37 °C for 1 h prior to photography at 100×.

In Vivo Studies—All experiments were approved by the Animal Studies Subcommittee and the Research and Development Committees at the Long Beach Veterans Affairs Medical Center. To determine the interactions of ANP and VPF *in vivo*, we utilized a transgenic mouse that overexpresses the ANP gene (44, 45). Founder mice were bred on a C3HeB/FeJ background to minimize the possibility of randomly segregating alleles. Non-transgenic littermates were used for comparisons, and PCR-based genotyping of tail DNA confirmed the identity of the mice. Plasma ANP levels in these mice are elevated compared with their non-transgenic littermates.

To determine permeability, a Miles assay (46) was adapted to mice. ANP transgenic or littermate control mice were anesthetized and intravenously injected with 100 μl of 0.5% Evan's blue dye. This was followed 30 min later by intradermal injection of either 10 μl of VEGF (1 μg/ml), 10 μl of 1 μM histamine, or saline, into the ears of the mice. In other experiments, HS-142-1 (1 μM), LY294002 (10 μM), wortmannin (50 nM), L-N^G-methyl-L-arginine acetate (10 μM), or PD98059 (1 μM) were co-administered with VPF. After 30 min, the mice were euthanized; the ears were photographed, and the injection site was carefully dissected to encompass the same amount of area from each mouse. The dye was then eluted from the dissected samples with formamide at 56 °C, and absorbance was quantitated by spectrophotometer (A_{600}). Injection site areas were also obtained from separate mice for kinase activity determination and were snap-frozen in liquid nitrogen. The samples were pulverized, followed by lysing in buffer containing protease inhibitors. Lysates were sonicated and microcentrifuged, and the resulting supernatants were immunoprecipitated for kinase studies.

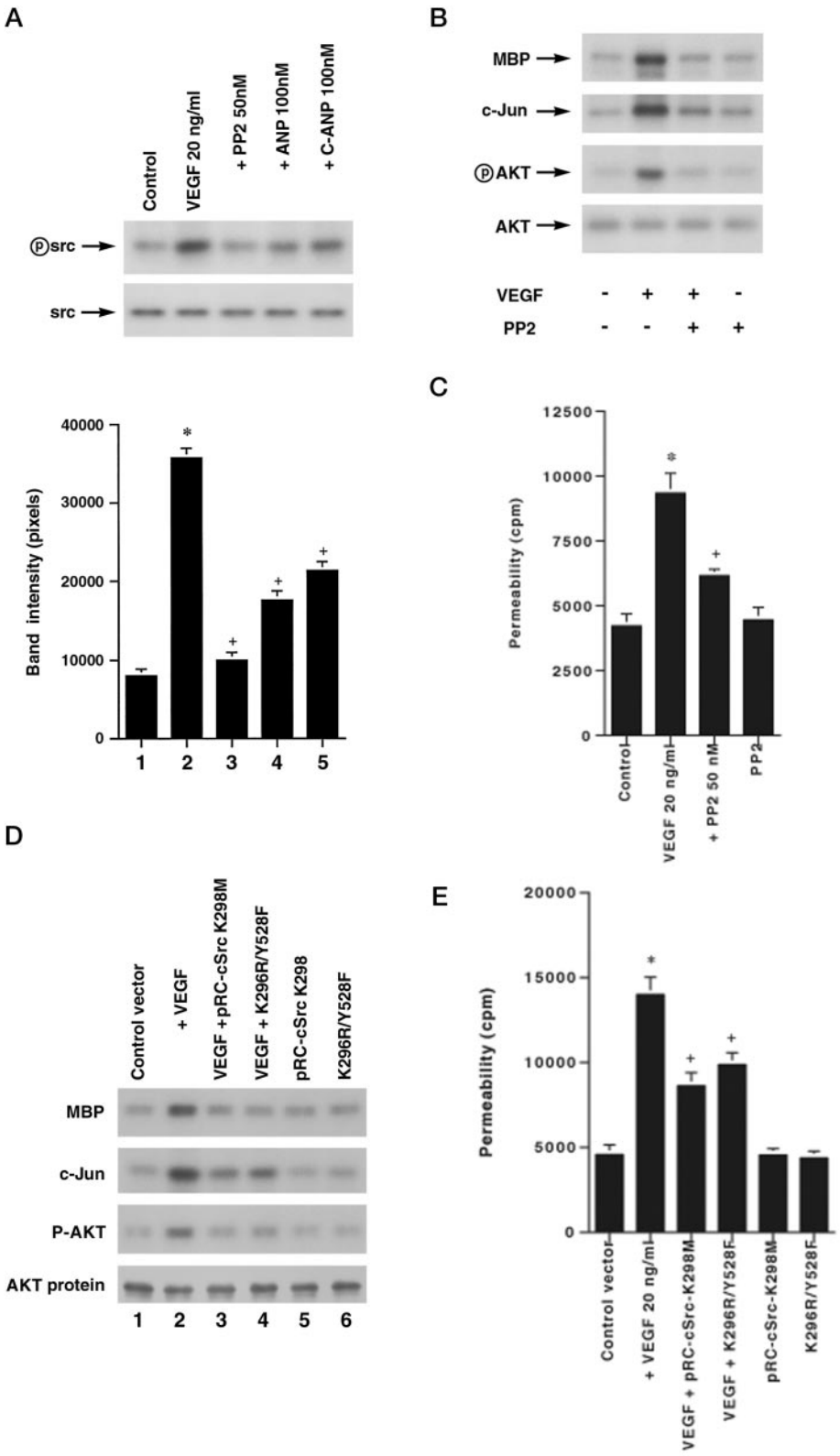

FIG. 1. **VPF signaling to permeability through Src.** *A*, VPF activates Src, inhibited by natriuretic peptides. BAEC were incubated for 8 min with VPF ± ANP, C-ANP-(4–23), or PP2, an antagonist of Src activation. Src phosphorylation at tyrosine 416 was determined by Western blot with a phospho-Src-specific antibody specific to this residue. Immunoblot of total Src protein is shown below a representative study. The *bar graph* represents three combined experiments, and the data were analyzed by analysis of variance plus Scheffe's test. *, $p < 0.05$ for control *versus* VPF; +, $p < 0.05$ for VPF *versus* VPF plus ANP or C-ANP-(4–23), or VPF + PP2. *B*, VPF activates ERK, JNK, and AKT via Src family kinases. EC were incubated with VEGF (VPF) ± PP2, and then ERK, JNK, and AKT activity/phosphorylation were determined as described under "Experimental Procedures." *MBP* is the protein substrate for ERK activity. Immunoblot of total AKT protein is shown below a representative study, repeated three times. *C*, Src family kinase(s) is necessary for VPF-induced permeability. EC in an upper chamber were incubated with VPF ± PP2 and [^{3}H]mannitol, and permeation was determined 24 h later. *Bar graphs* represent combined data from three experiments. Results are presented as counts/min of labeled mannitol in the lower chamber. *, $p < 0.05$ for control *versus* VPF; +, $p < 0.05$ for VPF *versus* VPF plus PP2. *D*, expression of dominant negative Src proteins abrogates VPF-induced ERK, JNK, and AKT kinase activity. EC were transiently transfected with dominant negative Src constructs pRC-cSrc-K298M or SrcK296R/Y528F and then recovered, synchronized, and incubated with or without VPF, and kinase activity was determined as for the PP2 studies. The data shown are representative of three experiments, and total AKT protein is shown below as a loading control. *E*, expression of mutant Src proteins inhibits VPF-induced permeability. Data are from three experiments combined. *, $p < 0.05$ for control *versus* VPF; +, $p < 0.05$ for VPF *versus* VPF + pRC-cSrc-K298M or Src-K296R/Y528F.

RESULTS

ANP Inhibits VPF-induced Src, through Both NPRC and GC Receptors—The non-membrane tyrosine kinase Src is critical to the participation of VPF in the vascular permeability/edema following cerebrovascular occlusion (17, 47). However, the signaling pathways downstream of Src that mediate permeability have not been defined. We first showed that VPF stimulates the activating phosphorylation of tyrosine 416 of Src and that ANP prevents this activation (Fig. 1*A*), as a potentially important function of the NP to inhibit VPF action. ANP can act at both GC-A receptors and the NPRC (28), but the VPF effect here was also significantly inhibited by C-ANP-(4–23), which only acts at the NPRC. These data therefore support both receptors as mediating the ability of ANP to inhibit Src activation, probably reflecting a common pathway downstream from each receptor.

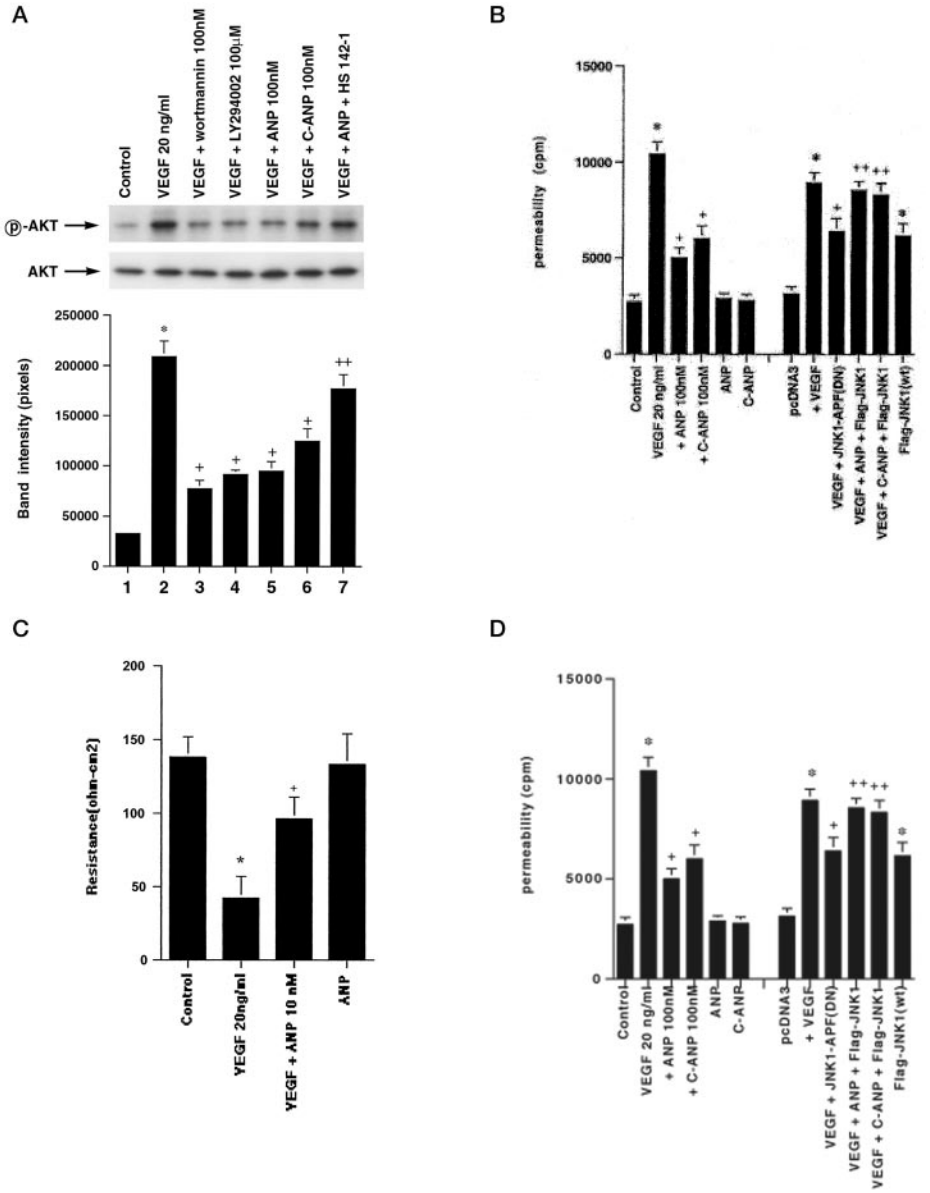

FIG. 2. **NP prevent VPF-induced activation of signaling to permeability AKT.** *A*, VPF-induced AKT occurs via PI3K and is prevented by NP. EC were exposed to VPF ± ANP or C-ANP-(4–23), with or without HS-142-1 for 15 min, and AKT activation was determined by Western blot, using phosphospecific antibody to serine 473. Other cells were co-incubated with VPF + wortmannin 100 nM, or LY2924002, 100 μM, and treated as above. The *bar graph* is composed from three separate studies. *, $p < 0.05$ for control *versus* VPF; +, $p < 0.05$ for VPF *versus* VPF plus ANP or C-ANP-(4–23), or PI3K inhibitors; ++, $p < 0.05$ for VPF + ANP *versus* same plus HS-142-1. *B*, permeability induced by VPF is blocked by ANP and C-ANP-(4–23) and is mediated by JNK. EC were incubated with VPF ± NP in non-transfected cells (control), or in cells transfected with pcDNA3 (2nd control), or a dominant negative Jnk-1 (APF), or constitutively active Jnk-1 (FLAG-JNK1), and permeability was determined. The data are from three experiments. *, $p < 0.05$ for control *versus* VPF or constitutively active JNK-1; +, $p < 0.05$ for VPF *versus* VPF plus ANP or C-ANP-(4–23), or JNK1 dominant negative; ++, $p < 0.05$ for VPF + ANP or C-ANP-(4–23) *versus* same plus FLAG-Jnk-1. *C*, electrical resistance of BAEC monolayers in response to VEGF ± ANP. EC monolayers were cultured on filters in Transwell until postconfluent, and then the cells were incubated under various conditions for 24 h. Resistance was determined as described under "Experimental Procedures." The studies were carried out three times, and the data was combined for the *bar graph*. *D*, PI3K and AKT underlie VPF-induced permeability. Control EC or cells expressing dominant negative AKT were incubated with VPF ± wortmannin or LY294003. *, $p < 0.05$ for control *versus* VPF; +, $p < 0.05$ for VPF *versus* VPF plus PI3K inhibitors or dominant negative AKT.

In response to cytokines, activated Src signals to the stimulation of numerous downstream kinases (48–50). To identify downstream effectors, we first validated the inhibitory function of the PP2 antagonist for the Src family of kinases (Fig. 1*A, lane 3*), and we then showed that VPF-induced ERK activation was dependent upon Src family kinase phosphorylation by using this inhibitor (Fig. 1*B*). Src family kinase activity was also important for VPF to stimulate JNK and PI3K/AKT activity in the EC because PP2 significantly prevented this. We showed previously (37) that VPF induces ERK-dependent JNK activation and subsequent angiogenesis *in vitro*, linking these signaling molecules. To establish the significance of Src here, we carried out permeability studies. As seen in Fig. 1*C*, PP2 significantly blocked the ability of VPF to stimulate labeled mannitol flux through the EC barrier by about 65%.

To corroborate the specific importance of Src, EC were transiently transfected to express two different and well validated kinase-deficient Src constructs (pRC-cSrcK298M (41) and K296R/Y528F (42)) that serve as dominant negative Src mutant proteins. The ability of VPF to stimulate ERK, JNK, and AKT activation was each very significantly impaired in this setting (Fig. 1*D*). We also carried out permeability studies and found that the mutant Src molecules significantly reduced VPF-induced EC permeability (Fig. 1*E*). These results identify and link downstream molecules that mediate VPF-induced permeability, emanating from Src activation.

Both JNK and PI3K Contribute to VPF-induced Permeability—We then determined the roles of JNK and PI3K/AKT, because these signaling molecules mediate other cellular effects of VPF (18, 51, 52). We recently showed that VPF significantly stimulates JNK activity in EC, and that is was inhibited maximally 69% by ANP or the NPRC-specific ligand, C-ANP(4–23). By using an antibody that detects the activating phosphorylation at serine 473 of AKT, we found here that VPF enhanced AKT activation nearly 5-fold (Fig. 2*A*). Activation of AKT was significantly blocked by the soluble PI3K inhibitors, wortmannin and LY294002, indicating that activation of PI3K occurred upstream of AKT augmentation. ANP blocked AKT activation by 70% (*lanes 2* and *5*), and this was substantially reversed by the GC receptor antagonist, HS-142-1 (53) (*lane 7*). C-ANP-(4–23) was less potent than ANP. These data support both the GC-A and NPRC as mediating the ability of ANP to inhibit AKT activation by VPF and indicate another level of restraint of permeability factor signaling.

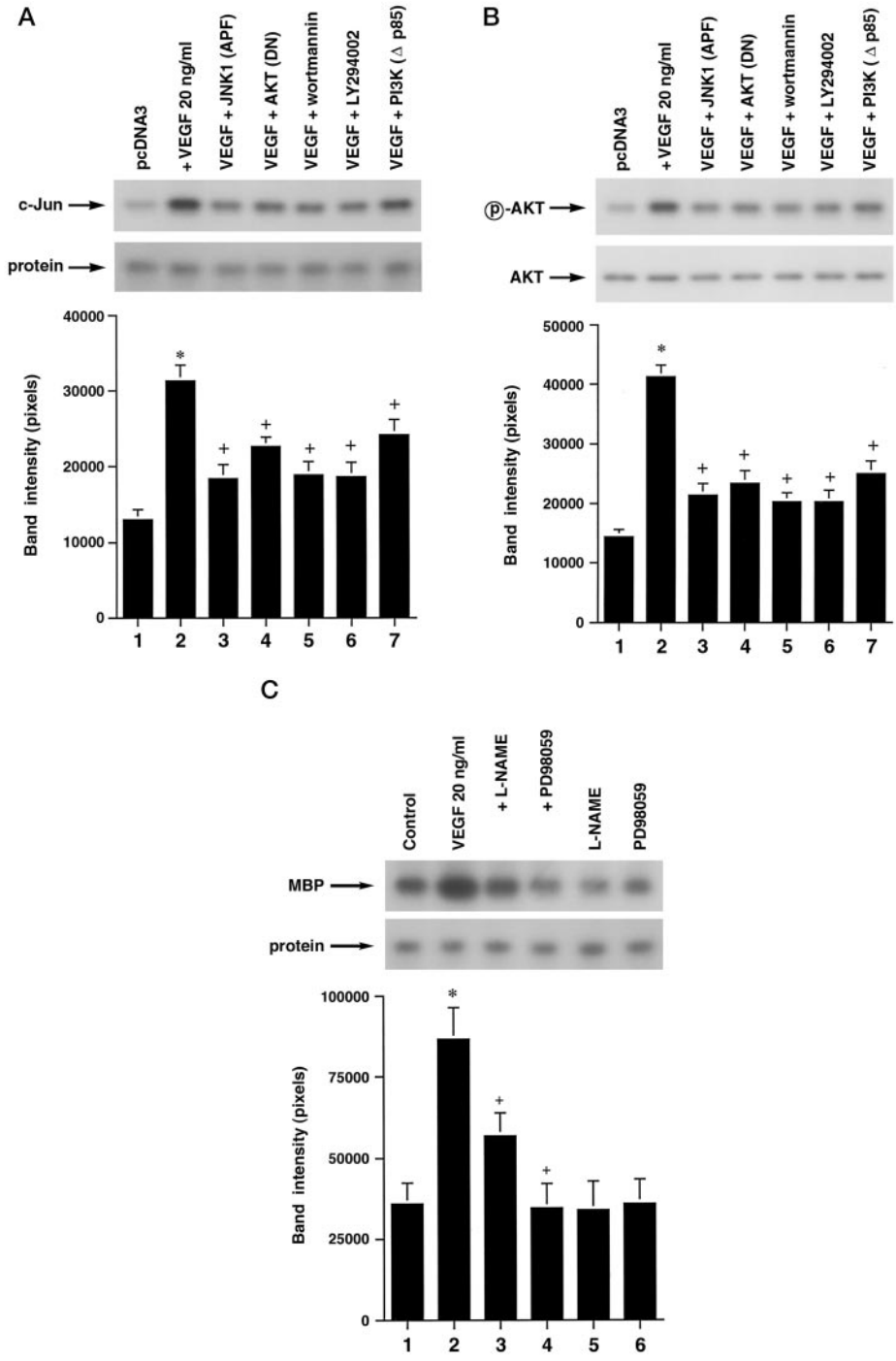

FIG. 3. **Cross-talk between PI3K/AKT and JNK.** *A*, VPF-induced JNK requires PI3K/AKT. EC were transfected with pcDNA3 (control), dominant negative AKT, or JNK1(APF), or Δp85 PI3K (dominant negative), and incubated with VPF ± wortmannin or LY294002. JNK activity was determined at 10 min, and total Jnk-1 protein is also shown. *, $p < 0.05$ for pcDNA3 *versus* VPF; +, $p < 0.05$ for VPF *versus* VPF+ condition, in three combined experiments. *B*, AKT activation by VPF is mediated through JNK and PI3K. EC were incubated with VPF ± wortmannin, LY294002, or transfected with Δp85 PI3K (dominant negative) or dominant negative AKT or JNK1(APF), and AKT activity was determined at 15 min. Total AKT protein is also shown. *, $p < 0.05$ for pcDNA3 *versus* VPF; +, $p < 0.05$ for VPF *versus* VPF+ condition, in three combined experiments. *C*, nitric oxide production precedes ERK activation by VEGF. EC were incubated with VEGF ± L-NAME, 1 μM, for 8 min, and ERK activity was determined. The study was repeated three times for the *bar graph*. *, $p < 0.05$ for control *versus* VEGF; +, $p < 0.05$ for VEGF *versus* VEGF plus L-NAME or PD98059.

We then asked whether these kinases contributed to VPF-induced EC permeability. In cultured cell monolayers, VPF caused a near 4-fold augmentation in permeability (Fig. 2*B, left side*). This was 70% blocked by ANP and, again, slightly less potently by C-ANP-(4–23). To implicate the involvement of JNK, we transiently expressed a dominant negative Jnk-1 (JNK1-APF) that we previously showed (37) was capable of preventing JNK activation, and which we validate here (Fig. 3). In this setting, VPF- induced permeability was 51% prevented (Fig. 2*B*, *right side*), and it must be considered that our transfection efficiency is only 52%. Therefore, the ability of ANP to block JNK activation (36) contributes to the inhibition of VPF-induced permeability by this natriuretic peptide. To support this idea, we transiently expressed a mildly constitutively active JNK-1 (FLAG-JNK1) (37, 38). As a result, ANP (or C-ANP-(4–23)) was significantly less capable of blocking VPF-induced permeability (Fig. 2*B*, *right side*). Thus, these data indicate the importance of this MAP kinase family member for ANP anti-permeability action. To confirm these results, the resistance to permeability was measured on the post-confluent EC monolayers (Fig. 2*C*). The basal resistance to permeability attributed to EC tight seal formation was 140 ohms/cm^2, and this was comparable with the resistance reported from microvascular EC (54). VEGF lowered resistance by 68%, and ANP significantly reversed the decreased permeability to VEGF.

A role for PI3K and AKT was examined. Wortmannin and LY294002 maximally inhibited VPF-induced permeability by 80 and 74%, respectively, indicating the importance of PI3K (Fig. 2*D*). To support the role of AKT, we transiently expressed a dominant negative AKT protein (37). Here VPF was 52% less

TABLE I
EC permeability in vitro in response to VPF

Data are from three combined experiments with duplicate determinations in each.

	Mannitol flux
	cpm
Control	4823 ± 122
VPF 20 ng/ml	9600 ± 230[a]
VPF + ANP 100 nM	6200 ± 191[b]
VPF + BNP 100 nM	6300 ± 204[b]
VPF + CNP 100 nM	6277 ± 186[b]
ANP	4794 ± 129
BNP	4688 ± 258
CNP	4856 ± 301
VPF + L-NAME 1 μM	6838 ± 292[b]
VPF + PD98059 10 μM	7388 ± 301[b]
VPF + SB203580 1 μM	7312 ± 277[b]
L-NAME	4894 ± 312
PD98059	4764 ± 189
SB203580	4694 ± 226

[a] $p < 0.05$ for control *versus* VPF.
[b] $p < 0.05$ for VPF *versus* VPF plus condition by analysis of variance plus Scheffe's.

potent in stimulating permeability, despite a 58% efficiency of dominant negative AKT transfection. Thus, PI3K/AKT are important effectors of VPF-induced permeability.

Cross-talk between JNK and PI3K—Our results implicate both JNK and PI3K/AKT as playing important roles in VPF-induced permeability. It is possible that the kinases act in distinct but complementary pathways to alter EC barrier function. Alternatively, JNK and PI3K/AKT may lie along the same signaling pathway, in response to VPF. To assess this, we first determined the role of PI3K and AKT in JNK activation. As seen in Fig. 3*A*, incubation of the cells with wortmannin, LY294002, or expression of a dominant negative PI3K p85 subunit (*lane 7*) each significantly inhibited VPF-induced JNK. Similarly, expression of the dominant negative AKT also prevented JNK activation by VPF (*lane 4*).

We then examined the phosphorylation of AKT. The ability of VPF to phosphorylate AKT was PI3K-driven, as shown using the dominant negative p85 subunit of PI3K, wortmannin, and LY294002 (Fig. 3*B*). Expression of the JNK1 APF construct also substantially prevented AKT activation (*lane 2 versus 3*). Validation of JNK1 (APF) to block endogenous JNK activation is also shown (Fig. 3*A*, *lane 3*). Thus, we provide novel evidence that these signaling molecules are linked in response to VPF, and this interaction may involve a bi-directional augmentory loop.

Several NP Block, Whereas NO and p38 Mediate, VPF-induced Permeability—We also determined the specificity of ANP to block VPF-induced permeability, in comparison to other NP family members. BNP functions similarly to ANP in that it binds both GC-A receptors and NPRC (28), and we found it to be equipotent to ANP for inhibiting this VPF action (Table I). Interestingly, CNP also significantly prevented VPF-induced permeability; this peptide binds a second guanylate cyclase receptor, GC-B, as well as NPRC, and thus is likely to act by mechanisms similar to that of ANP or BNP. ANP and BNP circulate after being secreted mainly from the heart, whereas CNP is produced in EC. Thus, all the members of this family of vasoactive peptides can inhibit VPF action, and these data complement our previous findings that several NP family members inhibit VPF synthesis (35).

From published cell models, NO is produced after VPF binds to Flk-1 (55, 56). Flk-1 ligation causes Src activation leading to NO production (57) and independently stimulates PI3K-dependent NO production (58). This leads to angiogenesis (58), and in part, NO-related ERK activation stimulates EC proliferation (59). NO production has also been implicated in VPF-induced permeability acting through unknown downstream targets (13). We found that the NO synthase inhibitor, L-NAME, partially but significantly (58%) blocked the ability of VPF to stimulate permeability. Additionally, the specific MEK inhibitor, PD98059, also partially blocked VPF-induced permeability (Table I), and NO inhibition partially prevented VEGF-induced ERK activation (Fig. 3*C*), linking these events. Finally, it has been reported that the p38 MAP kinase contributes to the ability of VPF to stimulate EC migration (60, 61). We found that upon using a specific and potent soluble inhibitor of p38, SB203580, VPF-induced permeability was partially blocked (Table I). Inhibiting either ERK or p38 MAP kinases resulted in a significant reduction of VPF-augmented permeability. Src-dependent ERK activation shown here provides upstream signaling for our previous report (37) that ERK activates JNK in response to VPF. Supporting this linkage, we found that VPF-induced JNK activity is also Src-dependent (Fig. 1*B*). These results further define the sequential signaling pathways involved in this specific function of the vascular growth/permeability factor.

VPF Stimulates ZO-1 and Occludin Phosphorylation via PI3K/Akt and JNK, Blocked by ANP—An important mechanism of EC barrier compromise is the disruption of the EC TJ. The ZO-1 protein maintains the structural integrity of TJ in both endothelial and epithelial cells. In response to VPF, we found that ZO-1 was strongly phosphorylated, using an antibody specific for serine/threonine residues (Fig. 4*A*). This was significantly prevented by the expression of JNK1(APF), dominant negative AKT, and by the PI3K inhibitors. Both AKT and JNK phosphorylate substrate Ser/Thr residues, and so the results are consistent with the known requirements of these kinases. The inhibition seen was not complete, and we cannot rule out the possibility of other Ser/Thr kinases playing a role. These results indicate that the specific kinases underlying VPF-induced permeability also phosphorylate ZO-1.

Because the phosphorylation of ZO-1 by VPF correlates with increased vascular permeability, then ANP might inhibit this function. We tested this idea, and we found that ANP (or C-ANP) inhibited ZO-1 phosphorylation by 55% (Fig. 4*B*). This partially resulted from GC-A activation, as the ANP effect was reversed by the specific guanylate cyclase inhibitor, HS-142-1 (*lane 5*), whereas the C-ANP inhibition was unaffected by this compound (demonstrating the involvement of the NPRC, as well). Our results point out a novel cross-talk activated by ANP binding the GC-A receptor, between cGMP/PKG and the inhibition of PI3K/AKT activation by the vascular permeability factor. ANP signaling through cGMP/PKG also inhibits JNK activation (see Ref. 36 and this work), and previous studies (62, 63) show that the relationship between cGMP and JNK is cell context-specific.

We next examined the possible phosphorylation of the TJ protein, occludin. As seen in Fig. 4*C*, VPF stimulated a 2.5-fold increased phosphorylation of this protein on Ser/Thr residues. This was significantly prevented by expressing dominant negative proteins for JNK (*lane 3*), AKT (*lane 4*), or by incubating the cells with wortmannin and LY294002 (*lanes 5* and *6*). Consistent with the signaling to permeability, and the phosphorylation of ZO-1 by VPF, ANP also caused a 74% inhibition of occludin phosphorylation (Fig. 4*D*). These effects were substantially prevented by the GC-A inhibitor (*lanes 3 versus 5*), but the NPRC receptor also contributed (*lane 4*).

Localization of ZO-1 and Occludin at the EC Tight Junction—Both occludin and ZO-1 proteins are crucial to the organization of the EC tight junction, and the two proteins physi-

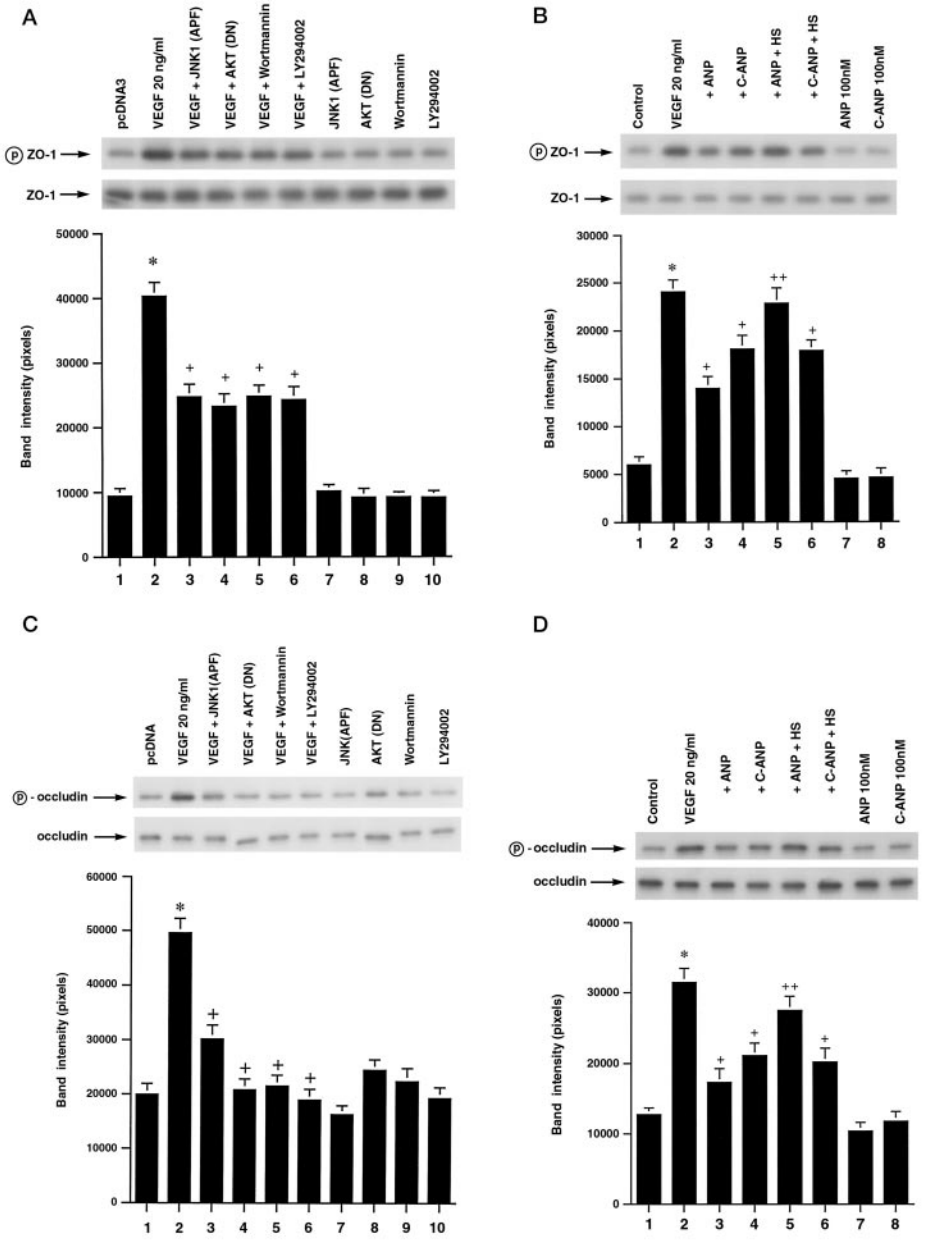

FIG. 4. **VPF induces the phosphorylation of ZO-1 and occludin proteins on threonine/serine residues.** *A*, VPF-induced ZO-1 phosphorylation is inhibited by dominant negative JNK, AKT, or soluble inhibitors of PI3K. *, $p < 0.05$ for pcDNA3 *versus* VPF; +, $p < 0.05$ for VPF *versus* VPF+ condition, in three combined experiments. Total ZO-1 protein is also shown. *B*, natriuretic peptides prevent VPF-induced phosphorylation of ZO-1 protein. EC were incubated with VPF ± NP (with and without the GC inhibitor HS 142–1). *, $p < 0.05$ for control *versus* VPF; +, $p < 0.05$ for VPF *versus* VPF+ condition. *C*, VPF-induced occludin phosphorylation is inhibited by dominant negative JNK, AKT, or soluble inhibitors of PI3K. *, $p < 0.05$ for pcDNA3 *versus* VPF; +, $p < 0.05$ for VPF *versus* VPF+ condition, in three combined experiments. *D*, natriuretic peptides inhibit VPF-induced phosphorylation of occludin. EC were incubated with VPF ± NP (with and without HS-142-1). *, $p < 0.05$ for control *versus* VPF; +, $p < 0.05$ for VPF *versus* VPF+ condition; ++, $p < 0.05$ for VPF and ANP *versus* VPF + ANP + HS-142-1.

cally associate with each other and with actin. By using immunohistochemistry, we identified the localization of ZO-1 at the EC cell contacts of confluent cells (Fig. 5*A*). The tightly organized and discrete localization of ZO-1 in the control cells (*panel a*) was in contrast to the disrupted localization and aggregation of this protein in response to VPF treatment (*panel b*). Expression of dominant negative JNK in the EC (*panel c*), dominant negative AKT (*panel d*), or wortmannin and LY294002 (*panels e* and *f*) each significantly prevented the effects of VPF. Thus, Ser/Thr phosphorylation of ZO-1 by the implicated kinases importantly contributes to the disruption of the TJ cytoarchitecture after VPF exposure, producing gaps at the EC interface boundary.

We also examined the effects of the natriuretic peptides (Fig. 5*B*). ANP or C-ANP substantially prevented the disruption of ZO-1 localization caused by VPF (*panels c* and *d*). Consistent with the roles of the GC-A and NPRC receptors, HS-142-1 partially but significantly reversed the effects of ANP (*panel e*) but not C-ANP-(4–23) (*panel f*). This identifies a cell biological effect of the NP to explain mechanistically how these peptides prevent increased vascular permeability due to VPF.

The localization of occludin in the EC barrier function was also determined by immunostaining (Fig. 5*C*). Occludin positioning in the EC contact points was severely disrupted by VPF (Fig. 5*C*, *panel b*), but this was prevented by expression of dominant negative Jnk-1 (*panel c*), dominant negative AKT (*panel d*), wortmannin (*panel e*), and LY294001 (*panel f*). In composite Fig. 5*D*, VPF disruption of occludin localization (*panel b*) is reversed by ANP (*panel c*) or C-ANP (*panel d*). The ANP effect was prevented by HS-142-1 (Fig. 5*D*, *panel e*), but the C-ANP action was not affected by the GC inhibitor (*panel f*). Furthermore, we showed that expression of dominant negative Src constructs (Fig. 5*E*, *panels c* and *d*) prevented VEGF-induced disruption of occludin localization (*panel b*). These results support a similar mechanism of VPF action directed toward both key TJ proteins.

VPF Signals to Actin Stress Fiber Formation That Is Prevented by ANP—The stability of actin association with TJ proteins contributes to the distinct cytoarchitecture that is necessary for EC barrier function (64). We therefore determined the effects of VPF signaling and the NP on actin organization. In control EC, there was a peripheral pattern of actin organiza-

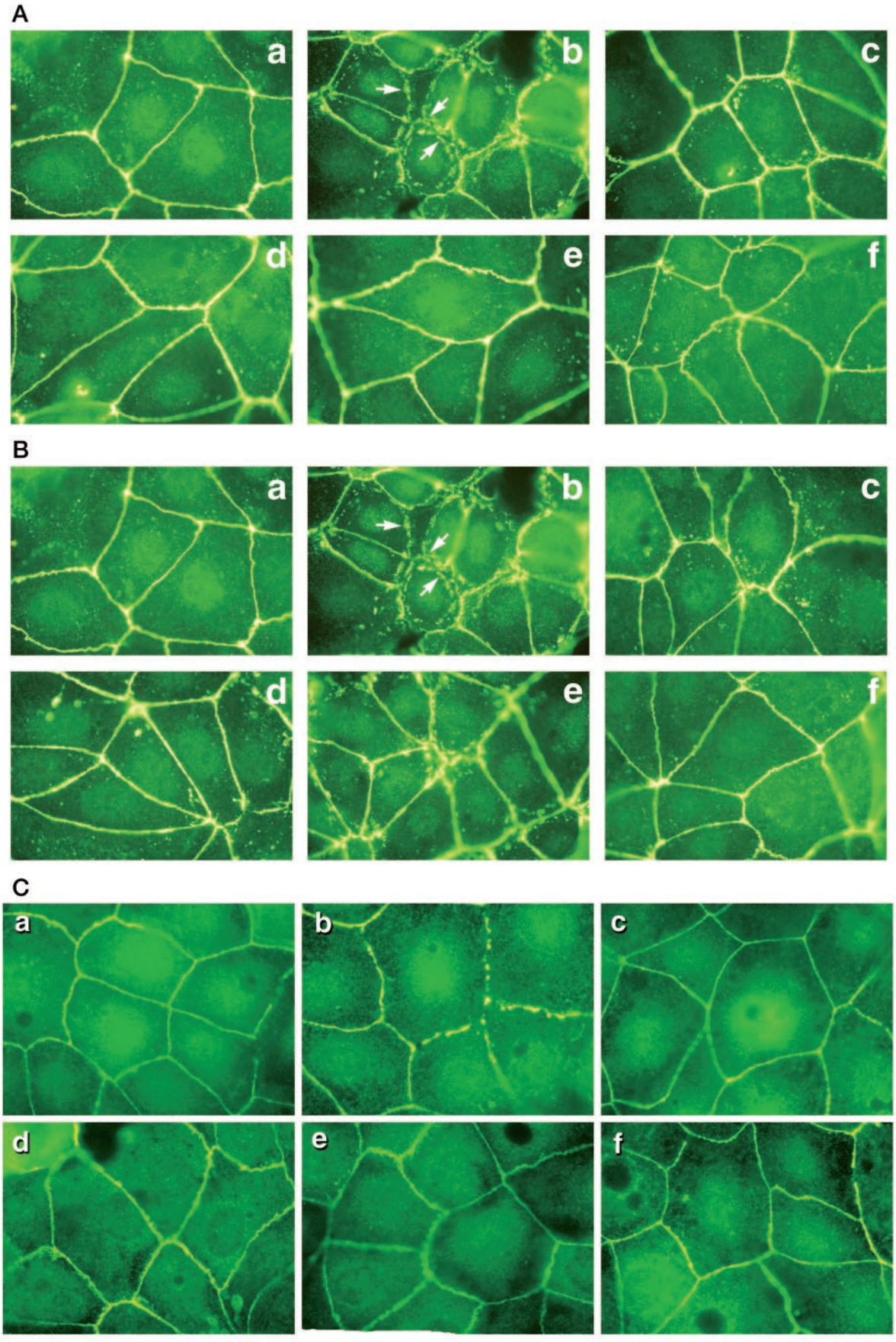

FIG. 5. **ZO-1 and occludin localization within the tight junction of endothelial cells is altered by VPF, which is inhibited by the natriuretic peptides.** *A*, the composite shows ZO-1 organization at the junctions of confluent EC, after staining with a specific antibody for this protein. *Panel a* is control EC; *panel b* is EC incubated with VPF 20 ng/ml; *panel c* is VPF added to cells expressing Jnk-1 APF (dominant negative);

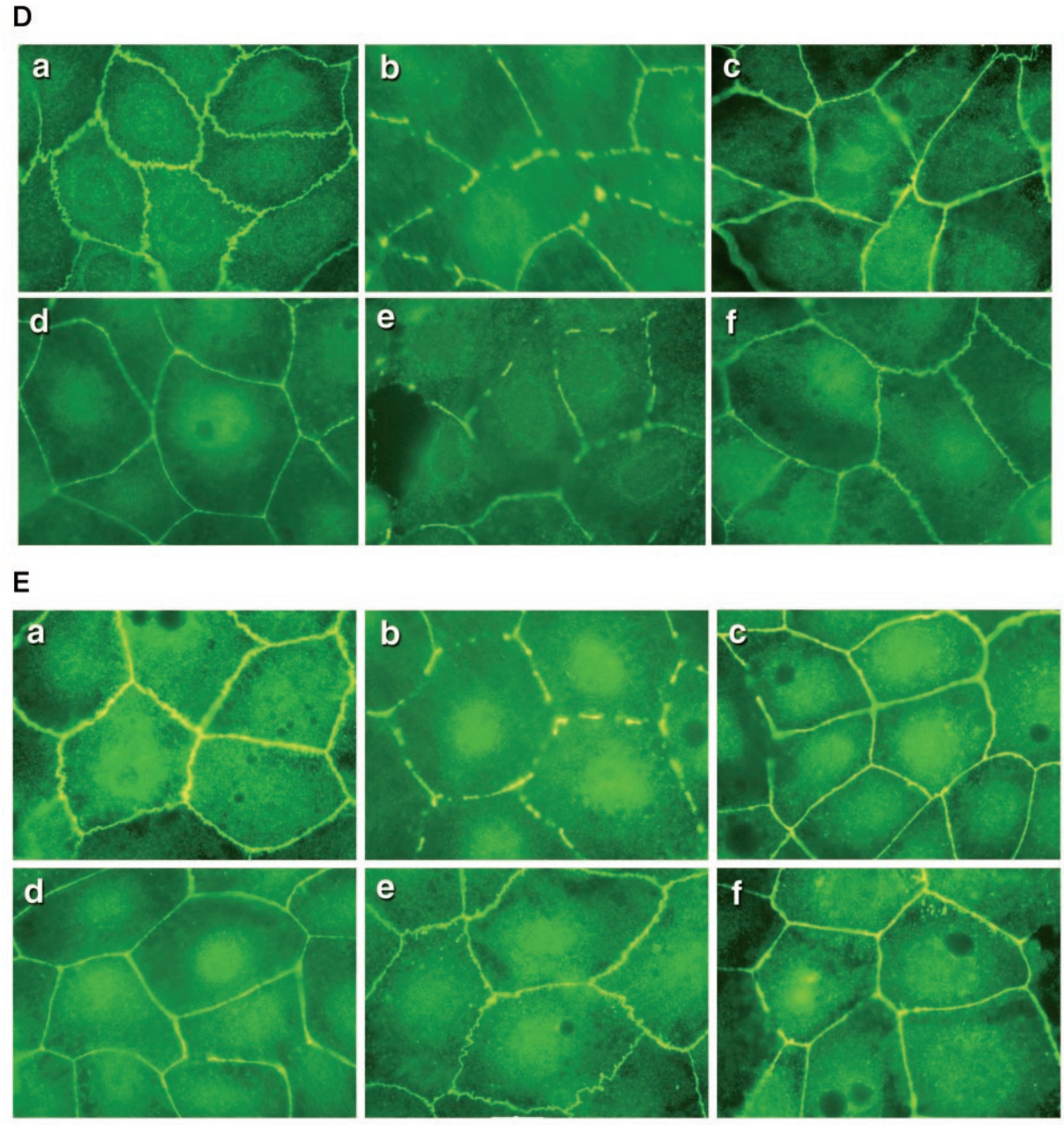

FIG. 5—*continued*

tion, characteristic of cells in an unperturbed state (Fig. 6*A*, *panel a*). VPF stimulated a re-arrangement of actin into stress fibers (Fig. 6*A*, *panel b*). When the cells were transfected with dominant negative JNK-1 and then incubated with VPF, there was a significant reversion of actin alignment toward the control situation (absence of VPF) (Fig. 6*A*, *panel c*). Similarly, expression of dominant negative AKT (Fig. 6*A*, *panel d*), or co-incubation of the cells with wortmannin (*panel e*) or LY294002 (*panel f*), prevented the majority of VPF-induced actin rearrangement. Consistent with the signaling data, ANP or C-ANP-(4–23) significantly prevented VPF-induced stress fiber formation (Fig. 6*B*, *panels a–d*). Blocking GC receptor

panel d is VPF added to cells expressing the AKT (dominant negative); *panel e* is VPF + wortmannin; and *panel f* is VPF + LY294002. The latter two inhibitors of PI3K had no effects by themselves (data not shown). *Arrows* show the disruption of the localization of these proteins at the apposition of the EC. *B*, the composite *panel a* is control; *panel b* is VPF; *panel c* is VPF + ANP 100 nM; *panel d* is VPF + C-ANP-(4–23) 100 nM; *panel e* is VPF + ANP + HS-142-1 (GC inhibitor); and *panel f* is VPF + C-ANP-(4–23) + HS-142-1. The NP or HS-142-1 by themselves had no effect. *C*, occludin localization is shown in control EC (*panel a*); *panel b* is EC incubated with VPF, 20 ng/ml; *panel c* is VPF added to cells expressing Jnk-1 (dominant negative); *panel d* is VPF added to cells expressing the AKT (dominant negative) protein; *panel e* is VPF + wortmannin; and *panel f* is VPF + LY294002. The latter two inhibitors of PI3K had no effect by themselves (data not shown). *D*, the composite is occludin staining in control EC (*panel a*); VPF-treated cells (*panel b*); VPF + ANP, 100 nM (*panel c*); VPF + C-ANP-(4–23), 100 nM (*panel d*); VPF + ANP + HS-142-1 (GC inhibitor) (*panel e*); and *panel f* is VPF + C-ANP-(4–23) + HS-142-1. *E*, control occludin localization (*panel a*) is altered by VPF (*panel b*); the effect is reversed by pRC-cSrc-K298M (*panel c*) or SrcK296R/Y528F expression (*panel d*). *Panels e* and *f* are the two dominant negative constructs alone. The composites are representative of three separate experiments.

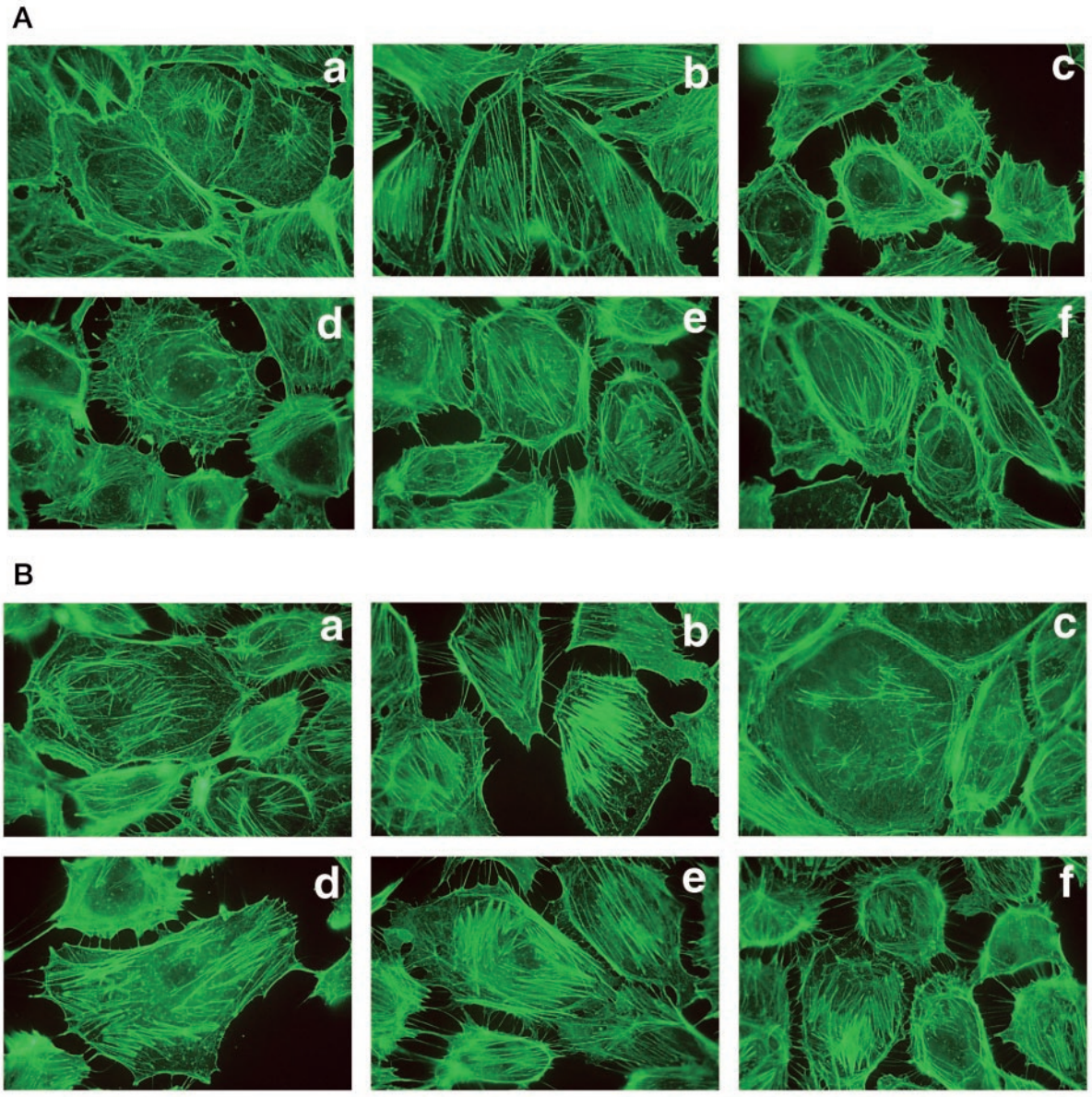

FIG. 6. **Actin rearrangement in the EC cytoskeleton is induced by VPF and is inhibited by the natriuretic peptides.** *A*, the composite shows actin organization in the EC, after staining with phyloiden. *Panel a* is control EC; *panel b* is EC incubated with VPF, 20 ng/ml; *panel c* is VPF incubated with cells expressing Jnk-1 APF (dominant negative); *panel d* is VPF added to cells expressing the AKT (dominant negative); *panel e* is VPF + wortmannin; and *panel f* is VPF + LY294002. The latter two inhibitors of PI3K had no effects by themselves (data not shown). *B*, the composite *panel a* is control; *panel b* is VPF; *panel c* is VPF + ANP, 100 nM; *panel d* is VPF + C-ANP-(4–23), 100 nM; *panel e* is VPF + ANP + HS-142-1 (GC inhibitor); and *panel f* is VPF + C-ANP-(4–23) + HS-142-1. The NP or HS-142-1 by themselves had no effect. The composites are representative of three separate experiments.

activation with HS-142-1 reversed the effects of ANP (Fig. 6*B*, *panels c versus e*) but had little effect on C-ANP-(4–23) action (*panels d versus f*). These results provide additional structural information relevant to the mechanisms by which VPF stimulates and the NP prevent EC permeability. Re-alignment of actin to stress fibers also importantly contributes to the ability of EC to migrate (65).

In Vivo Studies—To support our *in vitro* findings, we utilized a mouse that overexpresses an ANP transgene (44, 45). We confirmed that the plasma levels of ANP in these mice were significantly greater than their non-transgenic littermates plasma ANP 124 ± 0.8 *versus* 11.2 ± 0.2 pg/ml, $n = 4$ per group, $p < 0.05$). A Miles permeability assay (46) was then carried out to detect the interactions of ANP and VPF. Evans blue dye had been delivered by intravenous injection 30 min prior to VPF injection. Careful VPF injection into the ear skin of normal mice caused a rapid (10 s) and dense extravasation of dye (Fig. 7*A*, *left*). In contrast, the extravasation of dye upon VPF injection was significantly reduced in the ANP-overexpressing mice. Ear skin saline injections into either mouse was without effect. The quantification of these results is shown in Fig. 7*B* and indicates 65% less permeability to VPF in the ANP transgenic mice. The decreased response to VPF in the ANP-overexpressing mice was significantly reversed by the co- injection of the GC antagonist, HS-142-1, with VPF (Table II). Similarly, in both control and ANP-transgenic mice, inhibitors of PI3K, ERK, or NO partially prevented VPF-induced permeability. We also compared the effect of histamine injection, and we found that histamine-induced vascular permeability occurred comparably in normal or ANP transgenic mice (Fig. 7*A*, *right*).

Our *in vitro* data indicated the importance of VPF-induced kinase activation for permeability and that ANP inhibition of

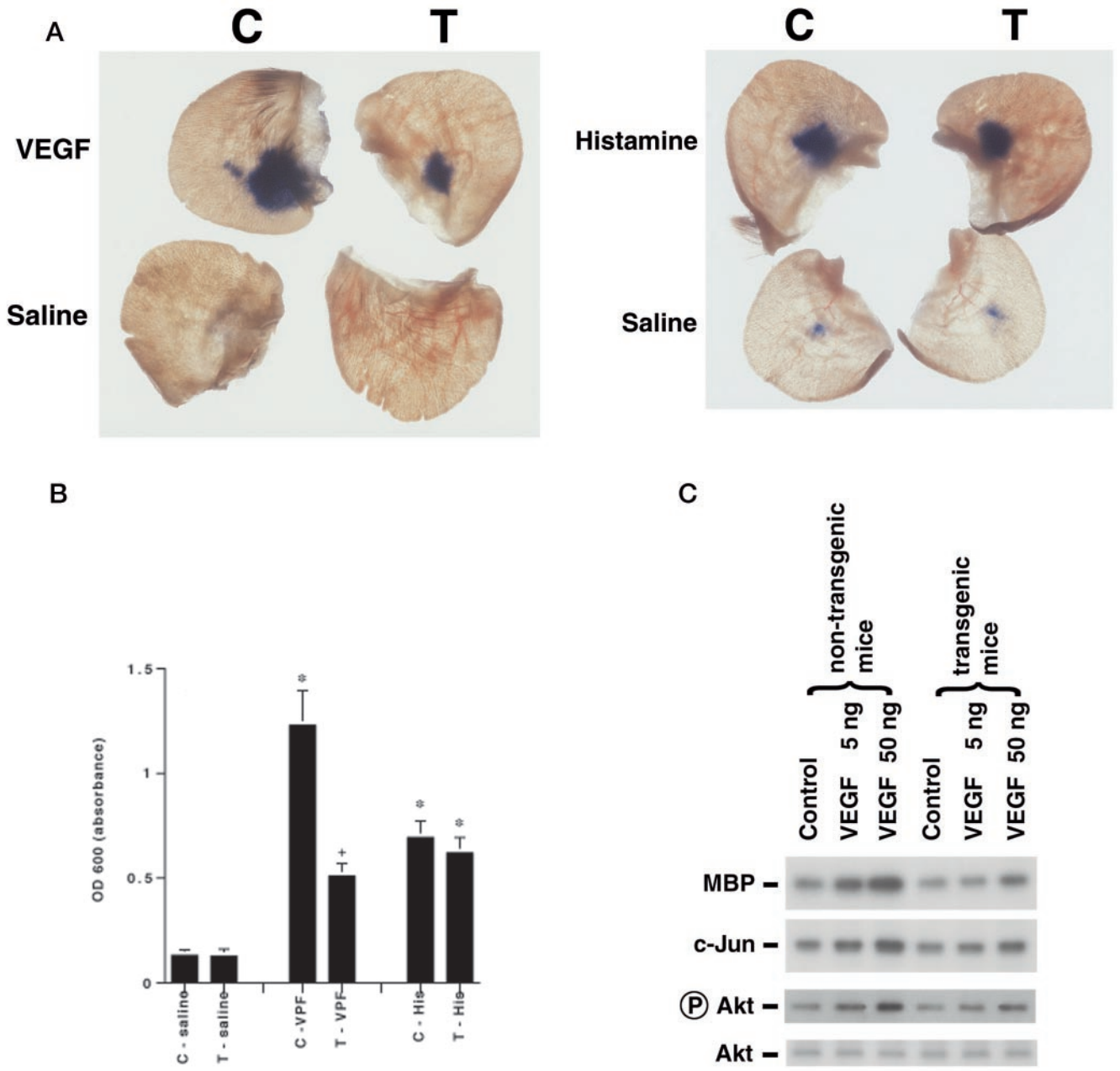

FIG. 7. **VPF-induced permeability is diminished in ANP-overexpressing mice.** *A*, Evans blue dye was intravenously administered 30 min prior to VPF or saline injection (*left*), or histamine or saline injection (*right*), delivered into the ear skin of ANP-transgenic mice or non-transgenic littermates ($n = 4$/condition). Representative photographs are shown. *B*, the density of dye resulting from VPF-induced permeability of carefully dissected areas of the skin was quantitated by a spectrophotometer. *, $p < 0.05$ for saline *versus* VPF or histamine; +, $p < 0.05$ for VPF in control mice (*C*) *versus* VPF in ANP-transgenic (*T*) mice. *C*, kinase activity extracted from the VPF injection site in ANP-transgenic or non-transgenic mice. Representative studies are shown, $n = 4–5$ mice per condition.

signaling provided a mechanistic understanding of the effects of this peptide. We therefore assessed the modulation of signaling at the VPF injection sites, in the transgenic and non-transgenic controls. VPF induced a clear increase in ERK, JNK, and AKT activity in normal mice (Fig. 7*C*). In contrast, VPF-induced kinase activation was markedly attenuated in the ANP-overexpressing mice. These data are quantified in Table III and provide *in vivo* support to the deduced mechanisms of VPF and ANP action.

DISCUSSION

VPF-induced vascular permeability is a critical contributor to the pathophysiology of diabetic retinopathy, ovarian, and other cancer-related ascites and the cerebral edema and injury following vascular insufficiency (1, 7, 8, 16, 17). Permeability of EC also contributes to angiogenesis. We report that the ability of VPF to modify 1) the actin cytoskeletal architecture, 2) TJ protein phosphorylation and localization, and 3) the permeability barrier function of vascular endothelial cells results from signaling. The tyrosine kinase activity of the Flk-1 receptor mediates the ability of VPF to signal to ERK and EC proliferation (59). Stimulation of the p38 MAP kinase or PI3K/AKT/S6 kinases by VPF underlies EC migration (54, 59, 60) and also proliferation (66). Interestingly, AKT can inhibit p38 kinase activation in some settings, thus promoting EC survival, a function of VPF (67). We showed previously that JNK (and molecules downstream from this kinase) affects VPF-induced cyclin D1 synthesis, Cdk4 activity, and G_1/S cell cyclin progression in EC (37). This occurs through a signaling cross-talk,

where ERK stimulation leads to the upstream activation of SEK-1 and JNK. Thus, multiple signaling proteins contribute to the various function of this important vascular factor.

Here we define the signaling events that are responsible for VPF-induced permeability and establish that the natriuretic peptides inhibit these functions (Fig. 7). VPF-induced Src is essential to the vascular permeability and cerebral edema that follows ischemic stroke (17, 47), but what occurs downstream of Src is not clear. We find that Src activation is necessary for VPF stimulation of ERK and JNK MAP kinases and the activation of PI3K/AKT (Fig. 8). By inhibiting each of these downstream proteins, we identify and link important signaling effectors of VPF and Src. These effectors result in the egress of molecules through the EC barrier. We also find that p38 MAP kinase and NO contribute to this effect of VPF. As shown previously, Flk-1 activation of Src results in enhanced NO production (57), and activation of endothelial nitric-oxide synthase contributes to VPF-induced angiogenesis and vascular permeability (68). Here we show that inhibition of NO generation partially prevents VEGF-induced ERK. It must be appreciated, however, that AKT can directly activate NO (69) upon activation by PI3K in response to VEGF (58).

We show that Src also activates JNK in the setting of VPF, and this occurs in part from ERK activation and ERK-JNK cross-talk (37). We report here a novel auto-activation loop for VPF signaling, where JNK and PI3K/AKT bi-directionally and positively regulate each other's activity. There is precedent that platelet-derived growth factor or epidermal growth factor activates a uni-directional cross-talk from PI3K to JNK (70). Analogous to our model, the small GTP-binding protein Rac has been found to be both upstream (71) and downstream of PI3K (72), leading to the proposal of a positive feedback loop between these two signaling proteins (71). These molecules are relevant to VPF action in that VPF-induced PI3K/AKT contributes to cell migration (18). The importance of JNK and PI3K/AKT cross-activation by VPF is demonstrated here in that signaling from these Ser/Thr kinases leads to alteration of 1) the morphological actin structure and TJ protein localization, and 2) enhanced permeability of the EC (see below). In diabetic proliferative retinopathy or the hypervascularity of prematurity, the newly formed blood vessels are "leaky," and this has been attributed in part to the actions of VPF, stimulated by hypoxic conditions in the retina (8, 73). Increased vascular permeability can lead to retinal hemorrhage and edema. Therefore, inhibition of the VPF-induced signaling that we define here (prevented in this case by natriuretic peptides) may be therapeutically useful.

How does VPF-induced signaling result in leaky EC? This permeability factor promotes fenestrations in EC and stimulates vesiculovascular organelle formation/function in venules (5, 6). VPF also promotes the paracellular transgression of fluid through EC tight junctions (3, 4). The important barrier function of EC is highly dependent upon the architecture of the TJ. TJ proteins such as the ZO family (ZO-1, -2, and -3) physically complex with occludin (74), claudin (75), junctional adhesion molecule (76), and cingulin (77), and several of these proteins associate with actin at cell junctions to form a seal (78). Rearrangement of the actin cytoskeleton disrupts the TJ protein(s) complex formation, lowering transcellular resistance and barrier function (23, 79). This also leads to the development of endothelial cell fenestrations that are known to be induced by VPF (6).

We found that after VPF treatment, a redistribution of ZO-1 and occludin proteins at the EC contact sites occurred, and this

TABLE II
Permeability response to VPF in normal or ANP-transgenic mice
Data are from four mice subjected to each treatment.

	Dye density ($A_{600\ nm}$)	
	Control mice	ANP transgenic mice
Saline	0.16 ± 0.03	0.19 ± 0.02
VPF 5 ng	1.40 ± 0.2[a]	0.62 ± 0.07[b]
VPF + HS-142-1	1.42 ± 0.2	1.10 ± 0.08
VPF + LY 294002	0.70 ± 0.2[c]	0.42 ± 0.06[c]
VPF + wortmannin	0.77 ± 0.09[c]	0.31 ± 0.04[c]
VPF + L-NMMA	0.82 ± 0.09[c]	0.51 ± 0.06
VPF ± PD98059	0.80 ± 0.06[c]	0.37 ± 0.002[c]

[a] $p < 0.05$ for saline *versus* VPF in control mice.
[b] $p < 0.05$ for VPF *versus* saline and control mice *versus* ANP-transgenic mice.
[c] $p < 0.05$ for VPF *versus* VPF plus condition as analyzed by ANOVA plus Schefe's test. Inhibitor compounds by themselves were no different than saline injection.

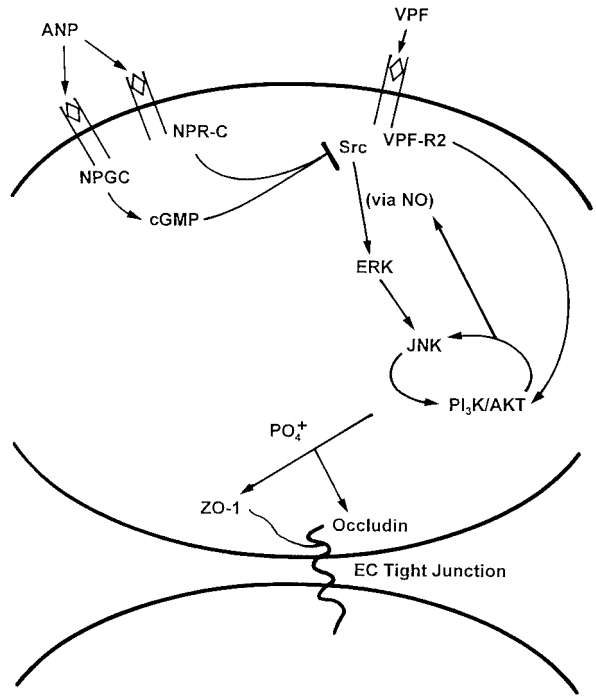

FIG. 8. **Schematic of VPF signaling to tight junction protein phosphorylation and vascular permeability, inhibited by natriuretic peptides.**

TABLE III
Kinase activation in response to VPF in normal or ANP-transgenic mice
Densitometry data are pooled specimens from four mice subjected to each treatment. C is control mice (non-transgenic), and T is transgenic mice. Data are densitometry units.

	Kinase activity (pixels ×1000)					
	ERK		JNK		AKT	
	C	T	C	T	C	T
Control (saline)	21.6	18.8	19.7	17.7	15.4	15.0
VPF 5 ng	35.7	19.6	24.8	19.8	26.6	17.9
VPF 50 ng	53.7	32.1	41.3	25.6	43.3	23.5

was blocked by ANP. It has been reported recently that VPF can 1) alter ZO-1 and occludin concentrations at the EC tight junction, and 2) lower transendothelial cell electrical resistance by undetermined mechanisms (80). Here we implicate the phosphorylation of these TJ proteins by JNK and PI3K/AKT, as the basis for the morphological alteration of the TJ. Preventing this phosphorylation by expressing dominant negative signaling molecules or by exposing the cells to ANP significantly led to the inhibition of VPF-enhanced permeability. Previous work (81) has implicated ERK in the increased EC permeability induced by VPF, which correlated with the loss of VE-cadherin and occludin localization at EC junctions. Also, oxidant stress induced by H_2O_2 causes ERK-dependent phosphorylation and redistribution of occludin in EC (27). In contrast, PKC induces serine phosphorylation of occludin, leading to the incorporation of occludin into the TJ of epithelial cells (82). Additionally, tyrosine phosphorylation of ZO-1 and occludin in EC occurs after exposure to VPF, induced by unknown kinases (24). There are numerous potential sites for JNK and AKT-induced Ser/Thr phosphorylation (as well as tyrosine) within ZO-1 and occludin, and a detailed mutagenesis study of the required residues for TJ assembly and VPF function is underway.

We also showed that VPF signaling through these pathways redistributes actin fibers in the EC. In part, this resulted from the generation of NO, which has been linked to ATP depletion, and the subsequent dilation of tight junctions (9, 21, 23). By contrast, ANP inhibits actin stress fiber formation, and VPF-induced permeability, enlarging the general role of natriuretic peptides to restrain pathological cardiac and vascular remodeling (reviewed in Ref. 28).

In support of this latter concept, GC-A knockout mice develop accelerated cardiac hypertrophy after aortic banding compared with normal littermates (84). As part of human congestive heart failure, ANP (and BNP) plasma levels are elevated 10-fold (85) and ANP may prevent deleterious cardiac remodeling or fibrosis (86). A concern is that chronically elevated NP in this setting might also impair compensatory new blood vessel formation during the recovery from ischemia-induced heart disease. However, these actions would be therapeutically desirable to prevent tumor angiogenesis and permeability, which are often VPF-dependent (87). CNP is another member of this protein family, and in our cell studies, ANP, BNP, and CNP were equipotent to inhibit VPF-induced permeability. Thus, the NP are unique as the only identified vascular peptides that inhibit both VPF production and action (51, 53). This is of interest in that the recently described anti-angiogenic properties of dopamine are selectively confined to reducing VPF receptor endocytosis and ligand binding (88).

The significance of the VPF-ANP interaction is supported by our *in vivo* findings. Transgenic mice overexpressing ANP demonstrated decreased capillary permeability and kinase activation following VPF administration. Co-administration of VPF with inhibitors of the ERK, PI3K, and c-Jun kinases confirmed their participation in VPF-induced permeability, and this was most evident in the non-transgenic mice. Importantly, ANP action is selective for VPF, as histamine-induced permeability was not meaningfully altered. ANP transgenic mice are known to have decreased blood pressure, compared with their non-transgenic littermates (43). However, this is unlikely to contribute to the anti-permeability effects of ANP we observe *in vivo*, because histamine-induced permeability was largely unaffected in transgenic mice.

The effects of ANP occur after binding to both GC and clearance (NPRC) receptors. The GC receptor generates cGMP and modulates most of the *in vivo* effects of ANP reported to date (83). We found that a specific GC antagonist, HS-142-1 (52), significantly prevented the effects of ANP but not the NPRC-specific ligand C-ANP-(4–23) both *in vitro* and *in vivo*. ANP inhibits VPF-induced Src activation and subsequent downstream signaling mainly through this mechanism, and this indicates a novel cross-talk where cGMP inhibits Src activation. Although the actions of ANP via cGMP are often mediated through activation of protein kinase G (PKG), it is not known whether the kinase or targets downstream from PKG might be important in this setting. We have found recently that a specific soluble inhibitor of PKGI substantially prevents the actions of ANP shown here.[2] Additionally, the signaling mechanisms for the NPRC are poorly understood but perhaps involve the inhibition of cAMP generation (reviewed in Ref. 28). The *in vivo* function of the NPRC is mainly to clear NP from serum (31), but it may contribute to other actions of ANP, as shown here.

In summary, we have defined a signal pathway that mediates the important function of VPF to induce vascular permeability. The signaling leads to the Ser/Thr phosphorylation and architectural disruption of protein components of the EC tight junction. Natriuretic peptides inhibit all these effects, thereby qualifying as potential anti-permeability factors. These results indicate unanticipated and potential therapeutic functions for the natriuretic peptides and are in concert with the roles of these peptides to dampen the response to and impact of insult to the cardiovascular system.

Acknowledgment—We thank Dr. Loren Field for providing breeding pairs of the ANP-overexpressing mice.

REFERENCES

1. Senger, D. R., Galli, S. J., Dvorak, A. M., Peruzzi, C. A., Harvey, V. S., and Dvorak, H. F. (1983) *Science* **219,** 983–985
2. Ferrara, N. (1993) *Trends Cardiovasc. Med.* **3,** 224–225
3. Milton, S. G., and Knutson, K. P. (1990) *J. Cell. Physiol.* **144,** 498–504
4. Larson, D. M. (1988) in *Endothethelial Function* (Ryan, U. S., ed) Vol. 3, pp. 75–84, CRC Press, Inc., Boca Raton, FL
5. Feng, D., Nagy, J. A., Hipp, J., Pyne, K., Dvorak, H. F., and Dvorak, A. M. (1997) *J. Physiol.* (*Lond.*) **504,** 747–761
6. Roberts, W. G., and Palade, G. E. (1995) *J. Cell Sci.* **108,** 2369–2379
7. Gossmann, A., Helbich, T. H., Mesiano, S., Shames, D. M., Wendland, M. F., Roberts, T. P., Ferrara, N., Jaffe, R. B., and Brasch, R. C. (2000) *Am. J. Obstet. Gynecol.* **183,** 956–963
8. Aiello, L. P., Avery, R. L., Arrigg, P. G., Keyt, B. A., Jampel, H. D., Shah, S. T., Pasquale, L. R., Thieme, H., Iwamoto, M. A., Park, J. E., Nguyen, H. V., Aiello, L. M., Ferrara, N., and King, G. L. (1994) *N. Engl. J. Med.* **331,** 1480–1487
9. Levin, E. R., Rosen, G. F., Yee, W., Cassidenti, D., Meldrum, D., and Pedram, A. (1998) *J. Clin. Invest.* **102,** 1978–1985
10. Millauer, B. S., Wizigmann-Voos, H., Schnurch, R., Martinez, N. P. H., Moeller, W., Risau, A., and Ullrich, A. (1993) *Cell* **72,** 835–846
11. Waltenberger, J., Claesson-Welsh, L., Siegbahn, A., Shibuya, M., and Heldin, C. H. (1994) *J. Biol. Chem.* **269,** 26988–26995
12. Soker, S., Takashima, S., Miao, H. Q., Neufeld, G., and Klagsbrun, M. (1998) *Cell* **92,** 735–745
13. Murohara, T., Horowitz, B. S., Silver, M., Tsurumi, Y., Chen, D., Sullivan, A., and Isner, J. M. (1998) *Circulation* **97,** 99–107
14. Stacker, S. A., Vitali, A., Caesar, C., Domagala, T., Groenen, L. C., Nice, E., Achen, M. G., and Wilks, A. F. (1999) *J. Biol. Chem.* **49,** 34884–34892
15. Guo, D., Jia, Q., Song, H.-Y., Warren, R. S., and Donner, D. B. (1995) *J. Biol. Chem.* **270,** 6729–6733
16. Van Bruggen, N., Thbodeaux, H., Plamer, J. T., Lee, W. P., Fu, L., Cairns, B., Tumas, D., Gerlai, R., Williams, S.-P., van Lookeren Campagne, M., and Ferrara, N. (1999) *J. Clin. Invest.* **104,** 1613–1620
17. Elicieri, B. P., Paul, R., Schwartzberg, P. L., Hood, J. D., Leng, J., and Cheresh, D. A. (1999) *Mol. Cell* **4,** 915–924
18. Radisavljevic, Z., Avraham, H., and Avraham, S. (2000) *J. Biol. Chem.* **275,** 20770–20774
19. Kroll, J., and Waltenberger, J. (1997) *J. Biol. Chem.* **272,** 32521–32527
20. Wu, H. M., Yuan, Y., Zawieja, D. C., Tinsley, J., and Granger, H. J. (1999) *Am. J. Physiol.* **276,** H535–H542
21. Clancy, R. M., Rediske, J., Tang, X., Nijher, N., Frenkel, S., Philips, M., and Abramson, S. B. (1997) *J. Clin. Invest.* **100,** 1789–1796
22. Salzman, A. L., Menconi, M. J. Unno, N., Ezzell, R. M., Casey, D. M., Gonzalez, P. K., and Fink, M. P. (1995) *Am. J. Physiol.* **268,** G361–G373
23. Bacallao, R., Garfinkel, A., Monke, S., Zampighi, G., and Mandel, L. J. (1994) *J. Cell Sci.* **107,** 3301–3313
24. Antonetti, D. A., Barber, A. J., Hollinger, L. A., Wolpert, E. B., and Gardner, T. W. (1999) *J. Biol. Chem.* **274,** 23463–23467

[2] A. Pedram, M. Razandi, and E. R. Levin, unpublished observations.

25. Staddon, J. M., Herrenknecht, K., Smales, C., and Rubin, L. L. (1995) *J. Cell Sci.* **108,** 609–619
26. Hirase, T., Kawashima, S., Wong, E. Y. M., Ueyama, T., Rikitake, Y., Tsukita, S., Yokoyama, M., and Staddon, J. M. (2001) *J. Biol. Chem.* **276,** 10423–10431
27. Kevil, C. G., Oshima, T., Alexander, B., Coe, L. L., and Alexander, J. S. (2000) *Am. J. Physiol.* **279,** C21–C30
28. Levin, E. R., Gardner, D. G., and Samson, W. K. (1998) *N. Engl. J. Med.* **339,** 321–328
29. Chang, M. S., Lowe, D. G., Lewis, M., Hellmiss, R., Chen, E., and Goeddel, D. V. (1989) *Nature* **334,** 68–71
30. Chinkers, M., Garbers, D. L., Chang, M. S., Lowe, D. G., Chin, H., Goeddel, D. V., and Schultz, S. (1989) *Nature* **338,** 78–83
31. Maack, T., Suzuki, M., Almeida, F. A., Nussenzveig, D., Scarborough, R. M., McEnroe, G. A., and Lewicki, J. A. (1987) *Science* **238,** 675–678
32. Itoh, H., Pratt, R. E., and Dzau, V. J. (1992) *Hypertension* **19,** 758–761
33. Levin, E. R., and Frank, H. J. L. (1991) *Am. J. Physiol.* **261,** E183–E189
34. Cuenda, A., Rouse, J., Doza, Y. N., Meier, R., Cohen, P., Gallagher, T. F., Young, P. R., and. Lee, J. C. (1995) *FEBS Lett.* 364, 229–233
35. Pedram, A., Hu, R.-M., and Levin, E. R. (1997) *J. Biol. Chem.* **272,** 17097–17103
36. Pedram, A., Razandi, M., and Levin, E. R. (2001) *Endocrinology* **142,** 1578–1586
37. Pedram, A., Razandi, M., and Levin, E. R. (1998) *J. Biol. Chem.* **273,** 26722–26728
38. Derijard, B., Raingeaud, J., Barrett, T., Wu, I. H., Han, J., Ulevitch, R. J., and Davis, R. J. (1995) *Science* **267,** 682–685
39. Khwaja, A., Rodriguez-Viciana, P., Wennstrom, S., Warne, P. H., and Downward, J. (1997) *EMBO J.* **16,** 2783–2793
40. Kong, M., Mounier, C., Wu, J., and Posner, B. I. (2000) *J. Biol. Chem.* **275,** 36035–36042
41. Luttrell, L. M., Hawes, B. E., van Biesen, T., Luttrell, D. K., Lansing, T. J., and Lefkowitz, R. J. (1996) *J. Biol. Chem.* **271,** 19443–19450
42. Simonson, M. S., Wang, Y., and Herman, W. H. (1996) *J. Biol. Chem.* **271,** 77–82
43. Hanke, J. H., Gardner, J. P., Dow, R. L., Changelian, P. S., Brissette, W. H., Weringer, E. J., Pollok, B. A., and Connelly, P. A. (1996) *J. Biol. Chem.* **271,** 695–701
44. Field, L. J., Veress, A. T., Steinhelper, M. E., Cochrane, K., and Sonnenberg, H. (1991) *Am. J. Physiol.* **260,** R1–R5
45. Steinhelper, M. E., Cochrane, K. L., and Field, L. J. (1990) *Hypertension* **16,** 301–307
46. Miles, A. A., and Miles, E. M. (1952) *J. Physiol.* (*Lond.*) **118,** 228–257
47. Paul, R., Zhang, Z. G., Eliceiri, B. P., Jiang, Q., Boccia, A. D., Zhang, R. I., Chopp, M., and Cheresh, D. A. (2001) *Nat. Med.* **7,** 222–227
48. Shono, T., Kanetake, H., and Kanda, S. (2001) *Exp. Cell Res.* **264,** 275–283
49. Timokhina, I., Kissel, H., Stella, G., and Besmer, P. (1998) *EMBO J.* **17,** 6250–6262
50. Encinas, M., Tansey, M. G., Tsui-pierchala, B. A., Comella, J. X., Milbrandt, J., and Johnson, E. M. (2001) *J. Neurosci.* **21,** 1464–1472
51. Tanno, S., Tanno, S., Mitsuuchi, Y., Altomare, D. A., Xiao, G. H., and Testa, R. C. (2001) *Cancer Res.* **15,** 589–593
52. Gerber, H. P., McMurtrey, A., Kowalski, J., Yan, M., Keyt, B. A., Dixit, V., and Ferrara, N. (1998) *J. Biol. Chem.* **273,** 30336–30343
53. Morishita, Y., Sano, T., Kase, H., Yamada, K., Inagami, T., and Matsuda, Y. (1992) *Eur. J. Pharmacol.* **225,** 203–207
54. Wang, W., Dentler, W. L., and Borchardt, R. T. (2001) *Am. J. Physiol.* **280,** H434–H440
55. Morales-Ruiz, M., Fulton, D., Sowa, G., Languino, L. R., Fuijo, Y., Walsh, K., and Sessa, W. C. (2000) *Circ. Res.* **86,** 892–896
56. Shen, B. Q., Lee, D. Y., and Zioncheck, T. F. (1999) *J. Biol. Chem.* **274,** 33057–33063
57. He, H., Venema, V. J., Gu, X., Venema, R. C., Marrero, M. B., and Caldwell, R. B. (1999) *J. Biol. Chem.* **274,** 25130–25135
58. Papapetropoulos, A., Guillermo-Cardena, G., Madri, J. A., and Sessa, W. C. (1997) *J. Clin. Invest.* **100,** 3131–3139
59. Parenti, A., Morbidelli, L., Cui, X. L., Douglas, J. G., Hood, J. D., Granger, H. J., Ledda, F., and Ziche, M. (1998) *J. Biol. Chem.* **273,** 4220–4226
60. Rousseau, S., Houle, F., Landry, J., and Huot, J. (1997) *Oncogene* **15,** 2169–2177
61. Rousseau, S., Houle, F., Kotanides, H., Witte, L., Waltenberger, J., Landry, J., and Huot, J. (2000) *J. Biol. Chem.* **275,** 10661–10672
62. Isono, M., Haneda, M., Maeda, S., Matsu-Kanbe, M., and Kikkawa, R. (1998) *Kidney Int.* **53,** 1133–1142
63. Komalavilas, P., Shah, P. K., Jo, H., and Lincoln, T. M. (1999) *J. Biol. Chem.* **274,** 34301–34309
64. Denker, B. M., and Nigam, S. K. (1998) *Am. J. Physiol.* **274,** F1–F9
65. Razandi, M., Pedram, A., and Levin, E. R. (2000) *J. Biol. Chem.* **275,** 38540–38546
66. Dayanir, V., Meyer, R. D., Lashkar, K., and Rahimi, N. (2001) *J. Biol. Chem.* **276,** 17686–17692
67. Gratton, J.-P., Morales-Ruiz, M., Kureishi, Y., Fulton, D., Walsh, K., and Sessa, W. C. (2001) *J. Biol. Chem.* **276,** 30359–30365
68. Fukumura, D., Gohongi, T., Kadambi, A., Izumi, Y., Ang, J., Yun, C.-O., Buerk, D. G., Huang, P. L., and Jain, R. K. (2001) *Proc. Natl. Acad. Sci. U. S. A.* **98,** 2604–2609
69. Fulton, D., Gratton, J. P., McCabe, T. J., Fontana, J., Fujio, Y., Walsh, K., Franke, T. F., Papapetropoulos, A., and Sessa, W. C. (1999) *Nature* **399,** 597–601
70. Logan, S. K., Falasca, M., Hu, P., and Schlessinger, J. (1997) *Mol. Cell. Biol.* **17,** 5784–5790
71. Coniglio, S. J., Jou, T.-S., and Symons, M. (2001) *J. Biol. Chem.* **276,** 28113–28120
72. Rodriguez-Viciana, P., Warne, P. H., Khwaja, A., Marte, B. M., Pappin, D., Das, P., Waterfield, M. D., Ridley, A., and Downward, J. (1997) *Cell* **89,** 457–467
73. Ferrara, N., and Davis-Smyth, T. (1997) *Endocr. Rev.* **18,** 4–25
74. Fanning, A. S., Jameson, B. J., Jesaitis, L. A., and Anderson, J. M. (1998) *J. Biol. Chem.* **273,** 29745–29753
75. Morita, K., Furuse, M., Fujimoto, K., and Tsukita, S. (1999) *Proc. Natl. Acad. Sci. U. S. A.* **96,** 511–516
76. Martin-Padura, I., Lostaglio, S., Schneeman, M., Williams, L., Romano, M., Fruscella, P., Panzeri, C., Stoppacciaro, A., Ruco, L., Villa, A., Simmons, D., and Dejana, E. (1998) *J. Cell Biol.* **142,** 117–127
77. Bazzoni, G., Martinez-Estrada, M., Orsenigo, F., Cordenonsi, M., Citi, S., and Dejana, E. (2000) *J. Biol. Chem.* **27,** 20520–20526
78. Wittchen, E. S., Haskins, J., and Stevenson, B. R. (1999) *J. Biol. Chem.* **274,** 35179–35185
79. Blum, M. S, Toninelli, E., Anderson, J. M., Balda, M. S., Zhou, J., O'Donnell, L., Pardi, R., and Bender, J. R. (1997) *Am. J. Physiol.* **273,** H286–H294
80. Wang, W., Dentler, W. L., and Borchardt, R. T. (2001) *Am. J. Physiol.* **280,** H434–H440
81. Kevil, C. G., Payne, D. K., Mire, E., and Alexander, J. S. (1998) *J. Biol. Chem.* **273,** 15099–15103
82. Andreeva, A. Y., Krause, E., Muller, E.-C., Blasig, I. E., and Utepbergenov, D. I. (2001) *J. Biol. Chem.* **276,** 38480–38486
83. Singh, S., Lowe, D. G., Thorpe, D. S., Rodriguez, H., Kuang, W. J., Dangott, L. J., Chinkers, M., Goeddel, D. V., and Garbers, D. L. (1988) *Nature* **334,** 708–712
84. Oliver, P. M., Fox, J. E., Kim, R., Rockman, H. A., Kim, H. S., Reddick, R. L., Pandey, K. N., Milgram, S. L., Smithies, O., and Maeda, N. (1997) *Proc. Natl. Acad. Sci. U. S. A.* **94,** 14730–14735
85. Wei, C. M., Heublein, D. M., Perrella, M. A., Lerman, A., Rodeheffer, R. J., McGregor, C. G., Edwards, W. D., Schaff, H. V., and Burnett, J. C., Jr. (1993) *Circulation* **88,** 1004–1009
86. Cao, L., and Gardner, D. G. (1995) *Hypertension* **25,** 227–234
87. Millauer, B., Shawver, L. K., Plate, K. H., Risau, W., and Ullrich, A. (1994) *Nature* **367,** 576–579
88. Basu, S., Nagy, J. A., Soumitro, P., Vasile, E., Eckelhoefer, I. A., Bliss, V. S., Manseau, E. J., Dasgupta, P. S., Dvorak, H. F., and Mukhopadhyay, D. (2001) *Nat. Med.* **7,** 569–574

MECHANISMS OF SIGNAL TRANSDUCTION:

Deciphering Vascular Endothelial Cell Growth Factor/Vascular Permeability Factor Signaling to Vascular Permeability: INHIBITION BY ATRIAL NATRIURETIC PEPTIDE

Ali Pedram, Mahnaz Razandi and Ellis R. Levin

J. Biol. Chem. 2002, 277:44385-44398.
doi: 10.1074/jbc.M202391200 originally published online September 3, 2002